Synthesis and Structural Analysis of $Ba_3V_2O_3S_4$

Frank Calvagna, Jianhua Zhang, Shoujian Li,† and Chong Zheng*

Department of Chemistry and Biochemistry, Northern Illinois University, DeKalb, Illinois 60115

Received April 27, 2000. Revised Manuscript Received September 14, 2000

A new quaternary barium vanadium oxysulfide, $Ba_3V_2O_3S_4$, was synthesized using the molten salt flux method. This solid-state compound crystallizes in the hexagonal space group $P6_3$ (No. 173) with $a = 10.1661(6)$ Å, $c = 5.9306(4)$ Å, $V = 530.81(6)$ Å^3, and $Z = 2$. It consists of face-sharing VS_6 octahedral chains and discrete VO_3S tetrahedra. The Ba atoms are located in the interstitial sites. Computational analysis indicates that this solid should be metallic as the conduction band in the vanadium d orbital region is partially filled.

Introduction

Rare-earth and transition metal oxysulfides are of great interest because of their potential applications in optical and electronic technologies.[1−6] Many ternary transition metal sulfides of the stoichiometry $A_xM_mS_n$ exist where A is an alkaline-earth metal and M a group 5 or 6 transition metal. These include $BaVS_3$, $Ba_{0.5}V_5S_8$, $Ba_9Nb_4S_{21}$, and the well-known superconducting Chevrel phases AMo_6S_8 (A = Sr, Ba).[7−10] However, not many quaternary oxysulfide compounds of this type are known. One example is $Ba_6V_4O_5S_{11}$ in which the structural building motifs are tetrahedral VS_4, VOS_3, and VO_2S_2 units.[11] In this contribution, we describe the synthesis, structural determination, and a computational study of a new quaternary compound $Ba_3V_2O_3S_4$ where the face-sharing VS_6 octahedra and isolated VO_3S tetrahedra are the main structural features.

Experimental Section

Synthesis of $Ba_3V_2O_3S_4$ was carried out using a molten KCl flux growth method. The KCl flux was previously dried at 250 °C under a vacuum over a period of 48 h. Handling of the KCl flux took place inside an Ar-filled glovebox. BaS (Allied Chemical) and elemental vanadium (Strem) were weighed in a 1:1 molar ratio (total of ≈0.5 g) and placed into a quartz ampule. Two grams of KCl flux was added to the reactant mixture. The quartz tube was evacuated to a pressure of $\approx 10^{-4}$ Torr and sealed. A computer-controlled furnace was used to heat the samples from 300 to 400 °C in 12 h and then from 400 to 800 °C in 12 h. The temperature of 800 °C was maintained for 72 h before cooling to 600 °C in 36 h and finally from 600 °C to room temperature in 12 h.

After the synthesis, many metallic needle crystals were observed in the sample. The oxygen content of the compound is due to residue oxygen in the quartz ampule and to contamination of the BaS starting material. Previous observation of this type of contamination in BaS has been made by Sutorik and Kanatzidis.[12]

Subsequently, optimized synthesis was carried out with the starting materials BaS, Ba, and V_2O_5 in the molar ratio of 4:1:1 (total amount 0.45 g) mixed with 2.0 g of KCl, using the same heating profile described above. The yield is larger, as much more needle crystals could be observed in the sample.

An EDAX analysis using the microprobe of a JEOL 35 CF-Kevex μx 7000 scanning electron microscope confirmed the presence of Ba, V, and S. The approximate ratio of the three elements in the same crystal used for the crystallographic study agreed with the crystallographically determined stoichiometry.

Several crystals of the compound were indexed on a Siemens SMART CCD diffractometer using 40 frames with an exposure time of 20 s/frame. All of them exhibited the same hexagonal lattice. One crystal with good reflection quality was chosen for data collection. A total of 3429 reflections were collected in the hemisphere of the reciprocal lattice of the hexagonal cell, of which 816 were unique with R(int) = 0.0534. An empirical absorption correction using the program SADABS[13] was applied to all observed reflections. The structure was solved with the direct method using the SHELXS and SIR97 programs;[13,14] both programs yielded the same structure. Full-matrix least-squares refinement on F^2 was carried out using the SHELXTL program.[13] The final agreement factor values are R1 = 0.0318 and wR2 = 0.0550 ($I > 2\sigma$). The final structure was checked for additional symmetry with the MISSYM algorithm[15] implemented in the PLATON program suite.[16] No additional symmetry was found. The unit cell information and refinement details are reported in Table 1. The atomic posi-

* To whom correspondence should be addressed. Telephone: (815) 753-6871. Fax: (815) 753-4802. E-mail: zheng@cz.chem.niu.edu.

† On leave from the Department of Chemistry, Sichuan University, Chengdu, Sichuan 610064, People's Republic of China.

(1) Sobon, L. E.; Wickersheim, K. A.; Buchanan, R. A.; Alves, R. V. *J. Appl. Phys.* **1971**, *42*, 3049.

(2) Alves, R. V.; Buchanan, R. A.; Wickersheim, K. A.; Yates, E. A. C. *J. Appl. Phys.* **1971**, *42*, 3043.

(3) Kaminskii, A. A. *Laser Crystals*; Springer-Verlag: Berlin, 1981.

(4) Smets, B., Smets, B., Eds.; Plenum: New York, 1991.

(5) Mamedov, A. A.; Smirnov, V. A. *Sov. Phys. Solid State* **1992**, *34*, 986.

(6) Blasse, G.; Grabmaier, B. C. *Luminescent Materials*; Springer-Verlag: Berlin, 1994.

(7) Gardner, R. A.; Vlasse, M.; Wold, A. *Acta Crystallogr. B* **1969**, *25*, 781.

(8) Petricek, S.; Boller, H.; Klepp, K. O. *Solid State Ionics* **1995**, *81*, 183.

(9) Saeki, M.; Onoda, M. *Bull. Chem. Soc. Jpn.* **1991**, *64*, 2923.

(10) Kubel, F.; Yvon, K. *Acta Crystallogr. C* **1987**, *43*, 1655.

(11) Litteer, J. B.; Fettinger, J. C.; Eichhorn, B. W. *Acta Crystallogr.* **1997**, *C53*, 163.

(12) Sutorik, A. C.; Kanatzidis, M. G. *Chem. Mater.* **1994**, *6*, 1700.

(13) Sheldrick, G. M. *SHELXTL. Version 5*; Siemens Analytical Instruments Inc.: Madison, WI, 1994.

(14) Altomare, A.; Burla, M. C.; Camalli, M.; Cascarano, G. L.; Giacovazzo, C.; Guagliardi, A.; Moliterni, A. G. G.; Polidori, G.; Spagna, R. *J. Appl. Crystallogr.* **1999**, *32*, 115.

(15) Le Page, Y. *J. Appl. Crystallogr.* **1987**, *20*, 264.

(16) Spek, A. L. *Acta Crystallogr., Sect. A: Found. Crystallogr.* **1990**, *46*, C34.

10.1021/cm000350k CCC: $20.00
Published on Web 01/05/2001

Table 1. Crystal Data and Structure Refinement for $Ba_3V_2O_3S_4$

formula weight	690.14
temperature	293(2) K
wavelength	0.71073 Å
crystal system	hexagonal
space group	$P6_3$
unit cell dimensions	$a = 10.1661(6)$ Å, $\alpha = 90°$
	$b = 10.1661(6)$ Å, $\beta = 90°$
	$c = 5.9306(4)$ Å, $\gamma = 120°$
volume	530.81(6) Å^3
Z	2
density (calculated)	4.318 Mg/m^3
absorption coefficient	13.404 mm^{-1}
θ range for data collection	2.31°−27.74°.
index ranges	$-11 \le h \le 13$, $-12 \le k \le 13$, $-6 \le l \le 7$
reflections collected	3429
independent reflections	816 [R(int) = 0.0534]
absorption correction	semiempirical from equivalents
max./min. transmission	1.000/0.606
refinement method	full-matrix least-squares on F^2
goodness-of-fit on F^2	1.206
final R indices [$I > 2\sigma(I)$][a]	R1 = 0.0318, wR2 = 0.0550
R indices (all data)	R1 = 0.0444, wR2 = 0.0604

[a] $R1 = \sum||F_o| - |F_c||/\sum|F_o|$; $wR2 = [\sum[w(F_o^2 - F_c^2)^2]/\sum[w(F_o^2)^2]]^{1/2}$.

Table 2. Atomic Coordinates ($\times 10^4$) and Equivalent Isotropic Displacement Parameters (Å$^2 \times 10^3$) for $Ba_3V_2O_3S_4$ (U(eq) Is Defined as One-Third of the Trace of the Orthogonalized U_{ij} Tensor)

	x	y	z	U(eq)
Ba	665(1)	3778(1)	6716(2)	15(1)
V(1)	0	0	4325(11)	12(1)
V(2)	−3333	3333	8130(5)	11(1)
S(1)	2108(2)	1756(2)	6829(7)	12(1)
S(2)	−3333	3333	4415(9)	22(1)
O	−3705(8)	4681(8)	9153(12)	19(2)

Table 3. Selected Bond Lengths (Å) and Angles (deg) for $Ba_3V_2O_3S_4$[a]

Ba−O#1	2.700(7)		
Ba−S(1)	3.0655(19)	S(1)#5−V(1)−S(1)#7	88.0(2)
Ba−O#2	3.078(7)	S(1)#5−V(1)−S(1)	179.9(3)
Ba−S(1)#3	3.1015(19)	S(1)#7−V(1)−S(1)	92.07(4)
Ba−S(2)#4	3.253(3)	S(1)−V(1)−S(1)#8	87.9(2)
V(1)−S(1)#5	2.479(5)	S(1)#5−V(1)−V(1)#6	126.67(14)
V(1)−S(1)	2.481(5)	S(1)−V(1)−V(1)#6	53.24(14)
V(1)−V(1)#6	2.96530(19)	O−V(2)−O#1	108.1(3)
V(2)−O	1.705(7)	O−V(2)−S(2)	110.8(3)
V(2)−S(2)	2.203(7)		

[a] Symmetry transformations used to generate equivalent atoms: (#1) $-x + y - 1, -x, z$; (#2) $-x, -y + 1, z - 1/2$; (#3) $-y, x - y, z$; (#4) $-x, -y + 1, z + 1/2$; (#5) $-x, -y, z - 1/2$; (#6) $-x, -y, z + 1/2$; (#7) $y, -x + y, z - 1/2$; (#8) $-x + y, -x, z$.

tions and equivalent isotropic displacement parameters are listed in Table 2. Selected bond lengths and angles are in Table 3.

Results and Discussion

Structure. $Ba_3V_2O_3S_4$ crystallizes in the hexagonal space group $P6_3$ (No. 173) with the lattice constants $a = 10.1661(6)$ Å, $c = 5.9306(4)$ Å, $V = 530.81(6)$ Å^3, and $Z = 2$. Figure 1 shows the $Ba_3V_2O_3S_4$ structure. It consists of chains of face-sharing VS_6 octahedra and discrete VO_3S tetrahedra. The face-sharing octahedral chain is observed in many ternary sulfide compounds such as $BaTiS_3$, $BaVS_3$, and $BaTaS_3$.[7,17,18] Because the sulfur atoms in each VS_6 octahedron are shared with an adjacent VS_6 octahedron, the stoichiometry for the octahedral chain is $VS_{6/2}$ or VS_3. The octahedral chains are parallel to the c axis, with two opposing faces shared with adjacent octahedra. These two faces are related by

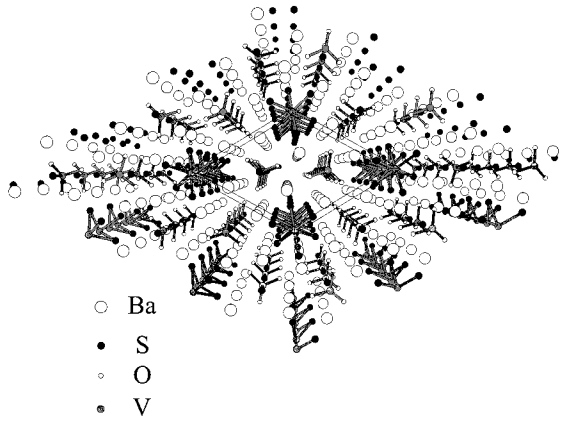

Figure 1. The $Ba_3V_2O_3S_4$ structure viewed down the c axis. The large open circles are Ba, the small open circles are O, the black circles are S, and the small shaded circles V.

the 6_3 screw axis. The discrete VO_3S tetrahedra and Ba ions separate these octahedral chains. The ratio of the Ba ion to the $VS_{6/2}$ octahedra and to the VO_3S tetrahedra is 3:1:1. Thus, the overall stoichiometry of the compound is $Ba_3V_2O_3S_4$. There are two formulas per cell because the translational repeating unit is two $VS_{6/2}$ octahedra due to the 6_3 screw symmetry. Because of a small distortion of the octahedron, there are two V to sulfur atom distances in the octahedron (V1−S1 in Table 3), 2.479(5) and 2.481(5) Å. The diagonal S1−V1−S1 angle is not exactly 180°, but 179.9(3)° (see **1**). The

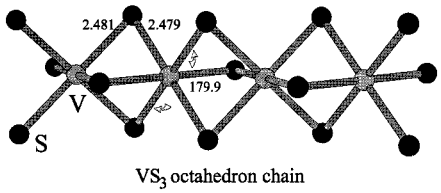

VS_3 octahedron chain

1

V−V distance is 2.9653(2) Å, slightly longer than the sum of the covalent radii of V (1.31 Å). The discrete VO_3S tetrahedron is also distorted, with three V2−O2 bond lengths equal to 1.705(7) Å and one V2−S2 length of 2.203(7) Å. The distorted tetrahedral angles, O−V2−S2 and O−V2−O angles, are 110.8(3)° and 108.1(3)°, respectively (see **2**). Finally, the coordination environ-

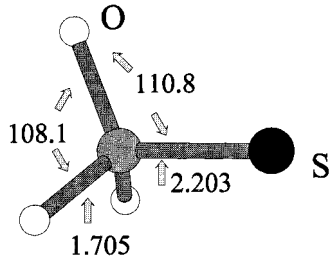

VO_3S tetrahedron

2

ment of the Ba atom is shown in **3**, where the seven

(17) Takano, M.; Kosugi, H.; Nakamura, N.; Shimada, M.; Wada, T.; Koizumi, M. *J. Phys. Soc. Jpn.* **1977**, *43*, 1101.
(18) Massenet, O.; Ruder, R.; Since, J. J.; Schlenker, C.; Mercier, J.; Kelber, J.; Stucky, G. D. *Mater. Res. Bull.* **1978**, *13*, 187.

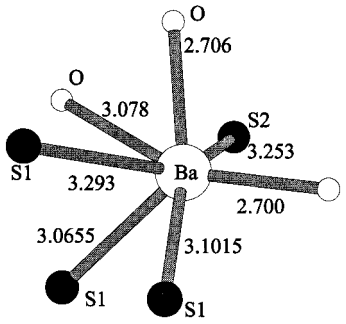

Coordination of Ba

3

atoms within 3.3 Å of the Ba atoms are plotted. The next shortest contact with the Ba atoms is at a distance of 3.412(4) Å, much larger than the sum of the covalent radii of Ba (2.17 Å) and S (1.03 Å).

Computational Analysis. To understand the bonding in the solid $Ba_3V_2O_3S_4$, we computed the density of states (DOS), band structure, and the crystal orbital overlap population (COOP) curves using the tight-binding extended Hückel method.[19−21] The parameters used in the computation are listed in Table 4. A set of 128 *k* points in the irreducible wedge of the Brillouin zone was employed in the computation of the DOS and COOP curves. The electronic structure of a transition metal at the center of a S_6 octahedron and of a tetrahedron is well-known. In an octahedral field, the metal d orbitals split into a lower t_{2g} and a higher e_g set. In the conventional coordinate setting, the *z* axis is parallel to a 4-fold rotation axis of the octahedron. But for a face-sharing octahedral chain, a more convenient coordinate setting is to choose the *z* axis parallel to the chain or pointing from the center to the face of the octahedron. The transformation between these two coordinate systems is well-known.[22−24] and is shown schematically in **4**. After the transformation, the d_{z^2} (*z*

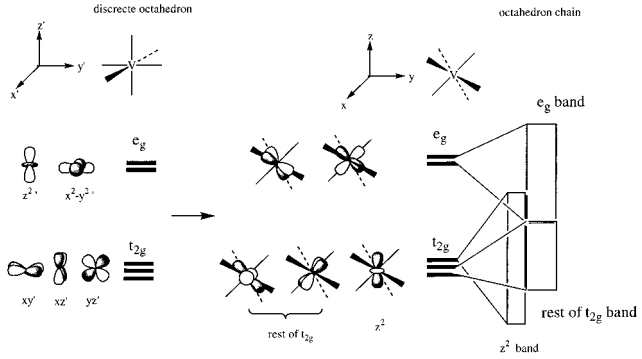

4

now parallel to the face-sharing octahedral chain) orbital belongs to the t_{2g} set. When the octahedra are packed to form a face-sharing chain, this orbital will develop into a band with largest dispersion among all d orbitals.

Table 4. Extended Hückel Parameters

	orbital	H_{ii} (eV)	ζ_1[a]	ζ_2	c_1[a]	c_2
Ba	6s	−7.0	2.2			
	6p	−4.0	2.2			
V	4s	−8.81	1.3			
	4p	−5.52	1.3			
	3d	−11.00	4.75	1.7	0.4755	0.7052
S	3s	−20.0	1.817			
	3p	−13.3	1.817			
O	2s	−32.3	2.275			
	2p	−14.8	2.275			

[a] Exponents and coefficients in a double ζ expansion of the d orbital.

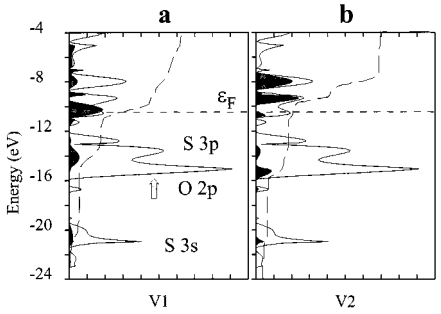

Figure 2. Computed DOS of $Ba_3V_2O_3S_4$. The shaded area is the individual contribution, the solid line the total DOS, and the dashed line the integrated individual contribution. The dashed horizontal line indicates the Fermi level. Panel (a): contribution from V1 (at the center of the octahedron). Panel (b): contribution from V2 (at the center of the tetrahedron).

Figure 2 shows the computed DOS where the shaded area is the individual contribution, the solid line the total DOS, and the dashed line the integrated individual contribution. The O 2s orbital is located around −34 eV and not shown in the figure. Those around −21 and −14 eV are the S 3s and S 3p orbitals. The oxygen 2p orbital is at the bottom of the broad peak between −12 and −16 eV. The peaks around the Fermi level are mainly vanadium d orbitals. Panel (a) shows the contribution of V1 (at the center of octahedra) to the total DOS. Because of the interaction with adjacent octahedra, the dispersion is larger compared to that of V2 (at the center of tetrahedra) in panel (b). The dispersion is also larger for S1 than for S2 as the discrete tetrahedra are separated from each other. The Fermi level cuts through the bottom of the vanadium d band, indicating metallic behavior of the compound. Although a d^1 configuration of vanadium is expected from a formal electron partition of $(Ba^{2+})_3(V^{4+})_2(O^{2-})_3(S^{2-})_4$, a more realistic electron configuration is $(Ba^{2+})_3V1^{3+}V2^{5+}(O^{2-})_3(S^{2-})_4$. This is because of the strong π-donor nature of the oxygen atom and the short V2−S distance. The extended Hückel calculation indeed showed a charge difference of +2 between V1 and V2, although the absolute charges were not correctly estimated ($V1^0$ and $V2^{+2}$) due to the well-known deficiency of the method.

Because of the interaction with neighboring cells, the d_{z^2} orbital at the octahedron center will have larger dispersion than the rest of the t_{2g} orbitals because it has better overlap with adjacent d_{z^2} orbitals. The same

(19) Hoffmann, R. *J. Chem. Phys.* **1963**, *39*, 1397.
(20) Whangbo, M.-H.; Hoffmann, R.; Woodward, R. B. *Proc. R. Soc. London* **1979**, *A366*, 23.
(21) Wijeyesekera, S. D.; Hoffmann, R. *Organometallics* **1984**, *3*, 949.
(22) Albright, T. A.; Hoffman, P.; Hoffmann, R. *J. Am. Chem. Soc.* **1977**, *99*, 7546.
(23) Orgel, L. E. *An Introduction to Transition Metal Chemistry*; Wiley: New York, 1969.
(24) Whangbo, M.-H.; Foshee, M. J.; Hoffmann, R. *Inorg. Chem.* **1980**, *19*, 1723.

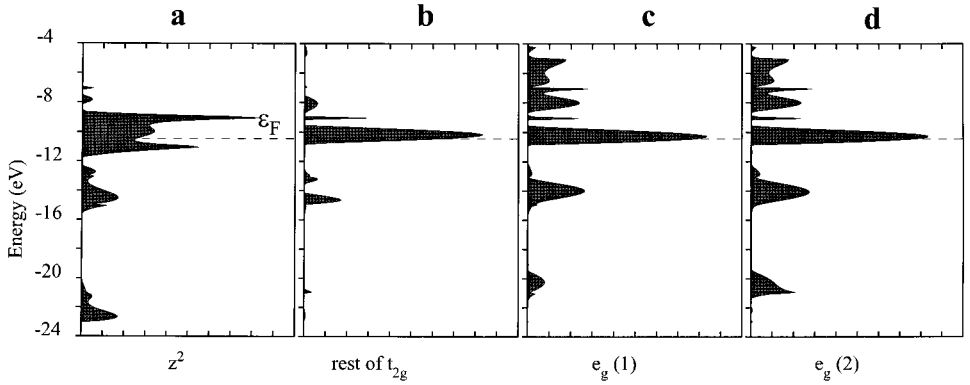

Figure 3. Computed DOS of $Ba_3V_2O_3S_4$. Panel (a): contribution of d_{z^2} (at the center of the octahedron). Panel (b): contribution from the rest of the t_{2g} set. Panel (c): contribution from one of the e_g sets (e_g1). Panel (d): contribution from e_g2.

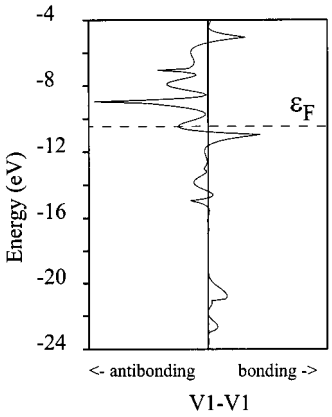

Figure 4. Computed COOP curve of the V1−V1 bond in the $Ba_3V_2O_3S_4$ structure. The dashed horizontal line indicates the Fermi level.

is true for one of the e_g orbitals as its lobes point toward the shared octahedral faces. The computed DOS, shown in Figure 3, confirms this observation. The two e_g orbitals, e_g1 and e_g2 (left and right e_g orbital in **4**), have the same extent of dispersion, as their lobes point toward the ligands.

Figure 4 shows the computed COOP curve of the V1−V1 bond. The curve demonstrates that the metal−metal interaction in the octahedral chain is mixed. At the bottom of the d band, it is bonding but at the Fermi level it is antibonding. The overall interaction, however, is nonbonding. The V1−V1 overlap population, which is the summation of the COOP values to the Fermi level, is 0.004. The metal−ligand interaction is mainly bonding below the Fermi level (not shown here). These features have been analyzed in detail by Whangbo, Foshee, and Hoffmann.[24]

It is interesting to notice that the sulfur−vanadium bond in the VO_3S tetrahedron is parallel to the *c* axis. Our computational analysis showed that this is due to the packing requirement in the cell. The channels where the VO_3S tetrahedra reside are narrow; the closest Ba−O contacts are at 2.70 and 2.71 Å. There is not enough room for sulfur atoms at these positions. If the sulfur atom in the VO_3S tetrahedron is replaced by an oxygen atom with a V−O distance of 1.705 Å, the closest Ba−O contact for this oxygen atom is at 3.525 Å, indicating that there is enough room for a sulfur atom at the axial position. The difference of the computed charges between these two types of oxygen atoms in this hypothetical structure is very small, −1.35 vs −1.31. Thus, the site preference is not electronic in origin. In the actual $Ba_3V_2O_3S_4$ structure, the closest Ba−S2 contact is at 3.253(3) Å, showing again that there is adequate space for the axial sulfur atom.

Conclusions

The group 5 transition metal quaternary sulfide compound $Ba_3V_2O_3S_4$ has been synthesized and analyzed. The computed band structure suggested that it should be metallic. Further study on the transport properties of the title compound will be carried out in the future once large enough crystals can be grown.

Acknowledgment. We thank the National Science Foundation for the support of our research through Grant DMR-9704048. We also thank Robert L. Bailey of the Department of Geology at Northern Illinois University for the assistance with the microprobe measurements.

Supporting Information Available: One X-ray crystallographic file (CIF) and tables of crystallographic information and structure factors are available (PDF). These are available free of charge via the Internet at http://pubs.acs.org.

CM000350K